Steel and Composite Structures, *Vol. 20, No. 5 (2016) 999-1022*
DOI: http://dx.doi.org/10.12989/scs.2016.20.5.999

Performance of steel beams strengthened with pultruded CFRP plate under various exposures

M. Gholami [*1], A.R. Mohd Sam [2a], A.K. Marsono [2], M.M. Tahir [3] and I. Faridmehr [3]

[1] *Road, Housing and Urban Development Research Center, Tehran, Iran*
[2] *Faculty of Civil Engineering, Universiti Teknologi Malaysia, Skudai, Malaysia*
[3] *UTM Construction Research Centre (CRC), Institute of Smart Infrastructures and Innovative Construction, Universiti Teknologi Malaysia (UTM), Skudai, Malaysia*

(*Received May 20, 2015, Revised December 29, 2015, Accepted January 03, 2016*)

Abstract. The use of Carbon Fiber Reinforced Polymer (CFRP) to strengthen steel structures has attracted the attention of researchers greatly. Previous studies demonstrated bonding of CFRP plates to the steel sections has been a successful method to increase the mechanical properties. However, the main limitation to popular use of steel/CFRP strengthening system is the concern on durability of bonding between steel and CFRP in various environmental conditions. The paper evaluates the performance of I-section steel beams strengthened with pultruded CFRP plate on the bottom flange after exposure to diverse conditions including natural tropical climate, wet/dry cycles, plain water, salt water and acidic solution. Four-point bending tests were performed at specific intervals and the mechanical properties were compared to the control beam. Besides, the ductility of the strengthened beams and distribution of shear stress in adhesive layer were investigated thoroughly. The study found the adhesive layer was the critical part and the performance of the system related directly to its behavior. The highest strength degradation was observed for the beams immersed in salt water around 18% after 8 months exposure. Besides, the ductility of all strengthened beams increased after exposure. A theoretical procedure was employed to model the degradation of epoxy adhesive.

Keywords: steel strengthening; steel/CFRP; environmental performance

1. Introduction

Steel structures constitute a large number of existing infrastructures which have been expanded all over the world and now reaching a critical age with increasing signs of deterioration and reduced functionality. Environmental deterioration, fatigue, and aging of structural elements are major problems in steel structures. Lack of proper maintenance and use of substandard materials in initial construction are other effective issues as well. Besides, many structures require upgrading to carry larger loads or should be retrofitted according to new codes.

Conventional methods of repair and retrofit of steel sections generally use steel plates through bolting or welding to the structure. Increasing considerable dead load to the structure,

*Corresponding author, Ph.D., E-mail: M.Gholami@bhrc.ac.ir
[a] Ph.D., E-mail: abdrahman@utm.my

http://www.techno-press.org/?journal=scs&subpage=6 ISSN: 1229-9367 (Print), 1598-6233 (Online)

susceptibility to the corrosion and need to heavy lifting equipment are some drawbacks of this method. In addition, welding is not a favorable solution due to fatigue problems. Further, mechanical details such as bolted connections which have better fatigue life are time consuming and costly.

The use of Fiber Reinforced Polymer (FRP) materials has been demonstrated as a successful technique to increase the strength and stiffness of structural elements. The superior mechanical and physical properties of FRP materials make them quite promising for repair and strengthening of structures and preferred to the steel plates. Several types of FRP are currently available to provide strength to metal structures. Lately researches showed Carbon Fiber Reinforced Polymer (CFRP) is considered to be the most suitable one for the purpose of strengthening of steel structures. This is essentially due to the higher stiffness of CFRP comparing to other types (Dawood and Rizkalla 2010).

A number of experimental and theoretical researches have been conducted to find the behavior of steel/CFRP bonding systems recently. Most of these studies concern to short term strengthening of steel sections. Bonding characteristics, flexural retrofit of beams, and fatigue improvement attracted more attentions. However, one of the main limitations to popular use of this technique has been the durability of bonding between steel and CFRP in various environmental conditions especially for the structures such as bridges which are exposed to natural environment (Gholami *et al*. 2013). Although previous studies emphasized CFRP strengthening method is quite acceptable, thorough researches need to be conducted to reveal long term durability problems.

This paper studies the performance of steel beams strengthened with pultruded CFRP plate after exposure to various environmental conditions. For this purpose, CFRP plate was bonded to the I-section steel beams on the bottom flange and the strengthened beams were placed under diverse aging exposures. The environmental conditions consisted of room ambient, natural tropical climate, wet/dry cycles, immersed in plain water, salt water, and acidic solution. The beams were subjected to the mentioned conditions up to 8 months. Then, four-point bending tests were carried out at specific intervals and the flexural behavior of the beams was evaluated. Maximum elastic load, flexural stiffness, ultimate load capacity, and maximum deflection were considered as the major mechanical properties in this study.

2. Background

Many experimental and analytical studies have already been carried out about strengthening structures using FRP materials. Most of these researches have concerned with concrete structures and the results demonstrated this technique has been implemented successfully. In contrast, using this technique for strengthening of steel structures has not gained the same popularity yet.

Strengthening of steel beams with CFRP plate commenced through research conducted at the University of North Florida by Sen *et al*. (1995). Further investigations indicated composite beams were successfully strengthened with CFRP strips and the mechanical properties increased between 20% and 50% (Sen *et al*. 2001). Mertz and Gillespie (2002) studied the full scale girders taken from demolished bridge and indicated the flexural stiffness of the repaired beams increased around 25%.

The study of using CFRP materials with different elastic modulus concluded the stiffness had to be similar or higher than steel to achieve appropriate strengthening performance (Al-Saidy *et al*. 2007). Moreover, the effect of CFRP bonding on the elastic stiffness of the beams was negligible

while on the plastic stiffness was remarkable (Colombi and Poggi 2006, Kabir and Eshaghian 2010). The behavior of steel beams strengthened with high modulus CFRP plates was investigated thoroughly (Schnerch *et al*. 2007) and a design guidelines was proposed for strengthening of composite bridge girder with HM CFRP. Similar studies concerned with the using CFRP strips on the web of steel beams and demonstrated the shear resistance of strengthened beams increased significantly (Patnaik *et al*. 2008, Narmashiri *et al*. 2010).

Repairing the steel beams which were notched intentionally at their tension flange was the concern of other studies as well (Kim and Brunell 2011, Zhou *et al*. 2013). The test results showed the elastic flexural stiffness and ultimate load carrying capacity of damaged beams exhibited remarkable increase, while the ductility reduced slightly. Besides, the steel/CFRP bonding characteristics was investigated by theoretical and numerical methods thoroughly (Deng and Lee 2007, Al-Zubaidy *et al*. 2013) as well as the effect of dynamic loads on the system (Colombi and Fava 2012). Finite element approaches were developed to model strengthened beams with CFRP plate on the bottom flange (Seleem *et al*. 2010, Narmashiri and Jumaat 2011) and the results indicated appropriate accordance to the experimental tests.

The most important environmental factors that influence the steel/CFRP system are temperature and moisture. In addition, wet/dry and freeze/thaw cycles, chemical attack and ultraviolet radiations (UV) may also affect it considerably. Obviously, a combination of the mentioned factors exists in natural environment and creates the worst situation for the system.

The adhesive layer between CFRP and steel is sensitive to high temperature. Consequently, the mechanical performance of steel/CFRP bonding system subjected to elevated temperature prevailed greatly by the adhesive (Nguyen *et al*. 2011). Indeed, subjecting to temperatures around the glass transition temperature of the adhesive causes the viscosity to increase rapidly and therefore, the strength and stiffness of joint reduce substantially.

The effect of temperature in adhesively bonded CFRP strengthening steel beams was studied by Stratford and Bisby (2012). The strengthened I-section steel beams were tested under combined temperature and load. First, the strengthened beams were loaded to the capacity of un-strengthened beam and then the temperature increased to failure of the specimens. Considerable joint slip appeared from around 40℃ before the plate debonded from the steel and it failed at a temperature of 65℃ which was the glass transition temperature of the adhesive. The results demonstrated the effect of CFRP plate bonded to steel beam can be significantly reduced by increasing the temperature.

Ingress of moisture to the steel/CFRP bonding joint is one of the major drawbacks of the plate bonding system (Landrock 2009). Normally, both the epoxy adhesive and CFRP matrix resin may be affected by the penetration of water into the bonded joint. In general, carbon fiber is impenetrable and moisture cannot affect it. In contrast, the FRP matrix resin is quite permeable and therefore, water absorption weakens the attraction between these two components. In addition, water absorption caused swelling leading to plasticization, a softening effect which reduced the shear strength of the polymer (Kumar *et al*. 2008).

It may take weeks to months before a substantial amount of moisture to be absorbed by adhesive (Dawood and Rizkalla 2010). Experimental tests demonstrated the moisture absorption increased very fast at the beginning of the immersion and then reached a constant level (Nguyen *et al*. 2012). However, the temperature of moisture influenced the amount of water uptake as well.

In addition, wet/dry and freeze/thaw conditions have been studied by Kim *et al*. (2012) recently. Double lap shear joints specimens were subjected to 100 cycles of wet/dry (8 h wet, 16 h dry) and freeze/thaw (8 h -20℃, 16 h room temperature) conditions. The average load carrying capacity

was found to be increased after exposure around 31% and 17% for wet/dry and freeze/thaw conditions, respectively.

The influence of relative humidity on epoxy adhesive was studied by Lettieri and Frigione (2012) and it was showed that large amount of water was absorbed when the humidity increased above 75%. Likewise, the effect of constant moisture and temperature (50℃; 93% RH) was investigated by Shan *et al*. (2011) using I-steel beams. The specimens consisted of two beams connected together with rotated steel hinge and CFRP sheets were bonded to the flanges. Further, a number of beams were subjected to flexural sustained loading around 30% of ultimate capacity during exposure. Bending tests were conducted after 15, 45, and 90 days and showed remarkable reduction of ultimate load carrying around 22%, 26%, and 57%, respectively. However, it was concluded the sustain loading had no significant influence on bond strength during exposure.

Generally, FRP materials have excellent resistance to corrosion and chemical attacks. However, the strengthening system using FRP may be affected in critical conditions. Salt water has been known as an aggressive chemical environment. A number of structures like bridges are subjected to salt water resulting from their use in coastal applications or due to exposure to de-icing salts. It was found the salt penetrated into the matrix and resulted in degradation different from that related to moisture alone (Cromwell *et al*. 2011). Further, recent studies suggested employing primer such as silane coupling agents had been helpful to postpone the steel corrosion (Dawood and Rizkalla 2010).

In addition, Nguyen *et al*. (2012) conducted a series of experimental test about durability of steel/CFRP double strap joints exposed to various conditions. Double lap joint specimens were submerged in salt water 5% at 20℃ and 50℃. The results demonstrated both stiffness and strength of the specimens degraded rapidly in the first 2 to 4 months of exposure. Moreover, a higher exposure temperature corresponded to a faster reduction, especially at the initial stage and the strength of joints reached at 85% and 74% of initial values for 20℃ and 50℃, respectively.

A review investigation was conducted by Gholami *et al*. (2013) and suggested the influence of natural environmental conditions must be studied to find the real behavior of the strengthening system. Besides, the effect of wet/dry condition and alkaline/acidic environment on the strengthening system needs more investigation.

Overall, little literature exists related to the performance of steel beams strengthened with CFRP plate under various environmental conditions. In this study, the experimental program was carried out to investigate the flexural behavior of strengthened beams after exposure to different environmental conditions including outdoor weathering, wet/dry cycles, immersed in plain water, salt water, and acidic solution. The beams were prepared and exposed to mentioned environments. Then, bending tests were conducted at specific intervals and the mechanical properties compared with control beam.

3. Experimental program

3.1 Material properties

The principal materials utilized in the experimental tests consisted of steel, CFRP plate and epoxy adhesive. These materials were tested individually based on appropriate ASTM standards to determine their mechanical properties. The results of the tests are presented in the following sections.

Table 1 Steel properties

Yielding tensile stress (MPa)	Young's modulus (MPa)	Ultimate tensile stress (MPa)	Ultimate tensile strain (mm/mm)
331.7	198.3	451.4	0.138

Table 2 Properties of CFRP plate

Source	Tensile strength (MPa)	Modulus of elasticity (GPa)	Ultimate elongation (%)	Fibre content (%)	Coefficient of expansion (m/m/℃)
Company	> 3100	170	2.00	68	0.6 × 10-6
Laboratory test	2850	158	1.81	-----	-----

3.1.1 Steel

I-sections steel beams were grade A36, type IPE 100A. The tensile properties of the steel were identified based on ASTM A370 (2012) using dog-bone steel coupons which were cut from the original material. The tensile test was conducted using Universal Tensile Machine (DARTEC) with the capacity of 200 kN with a constant displacement rate of 1 mm/min. The average mechanical properties extracted from the tests are presented in Table 1.

3.1.2 CFRP plate

The pultruded CFRP plate was employed named "Carboplate" produced by "Mapei" Company. The strips packaged as 100-meter long rolls, with a width of 50 mm and thickness of 1.4 mm. In order to find the mechanical properties, the CFRP coupons were prepared and tested according to ASTM D3039 (2008). Table 2 presents the properties of the CFRP plate from the laboratory test and the one mentioned by the company. To assess the effect of environmental exposure on the mechanical properties of individual CFRP material, additional coupons were environmentally conditioned and tested to failure subsequently.

3.1.3 Epoxy adhesive

A two part epoxy adhesive produced by "Mapei Company" named "Adesilex PG2" was used to bond the CFRP plate to the steel surface. This adhesive was recommended by the manufacturer to use with "Carboplate" for their compatible behavior. In addition, dog-bone coupons were prepared and tested based on ASTM D638 (2010) to measure the mechanical properties of the adhesive individually. The epoxy adhesive coupons were tested in tension using a 25 kN Instron machine. The properties of epoxy adhesive from the lab tests and the one presented by the company are given in Table 3.

Table 3 Properties of epoxy adhesive

Source	Tensile strength (MPa)	Modulus of elasticity (GPa)	Ultimate elongation (%)	Shearing strength (MPa)	Coefficient of expansion (m/m/℃)	Glass transition temperature (℃)
Company	> 18	-----	-----	> 28	46×10^{-6}	> 40
Laboratory tests	19.5	11.5	0.199	-----	-----	-----

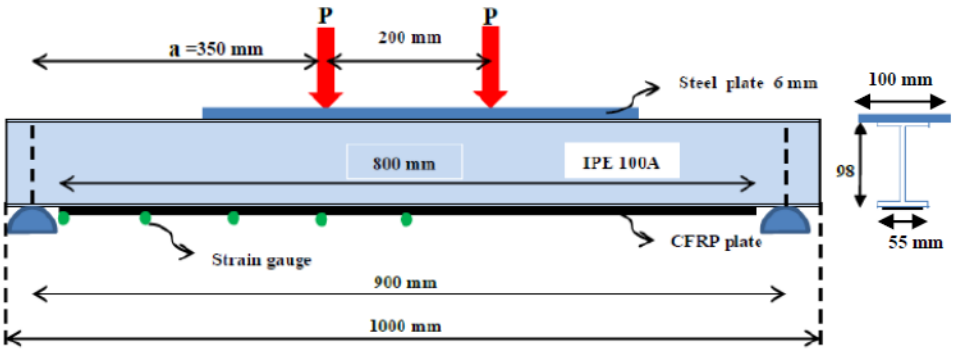

Fig. 1 Geometry of I-section steel beams strengthened with CFRP plate

3.2 Beams geometry

A total number of 35 I-section steel beams with the length of 1000 mm were used to study the flexural behavior of strengthened beams. Fig. 1 demonstrates the geometry of the I-section strengthened beams. Spherically seated supports were located at 50 mm from the ends of the beam. The CFRP plate with the dimension of 1.4 × 50 × 800 mm were bonded to the tension flange of the beams using epoxy adhesive which nearly covered the entire width of bottom flange. Steel surface preparation is one of the most important steps governing the quality of bonding. Proper surface treatment of steel produces a rough surface free from contamination and enhances the formation of chemical bonds between steel and the adhesive. The best method recommended for cleaning steel surface is sandblasting (Hollaway 2010). Hence, this technique was used to remove all the rust, oil and contamination from the surface of the bottom flanges. In addition, the flanges were completely cleaned with vacuum cleaner and acetone from any dust to provide a suitable active surface for chemical bonding.

Moreover, an additional 6 mm thick steel plate was welded to the compression flange along its length to prevent compression failure or premature buckling at the top flange. Obviously, this issue shifted the neutral axis of the beam section towards the compression flange and caused more tensile stress to be created at the bottom flange which increased the shear stress along the bonding system preferably.

3.3 Environmental conditions

Diverse environmental conditions have been chosen according to ASTM D1828 to investigate the effect of different factors on the behavior of the bonding system. The overall scenarios for environmental conditions are given in Table 4. The duration of all conditions was considered as 8 months due to the available time limit of the research. A number of 5 beams were used for short term and room ambient condition and the other beams were exposed to scenarios A to E (2 beams for each duration). The room ambient was considered as a condition which had minor effects. The temperature and relative humidity in this condition was measured between 25-28℃ and 70-90% RH, respectively. The environmental condition in scenario (A) was natural tropical climate at the southern of Malaysia. The aim of this scenario was to evaluate the properties of the specimens subjected to a harsh natural exposure. In this scenario the combination of environmental effects including high temperature and humidity, wet/dry and thermal cycles, and sunlight ultraviolet

Table 4 Environmental exposures

Scenarios	Specimens	Environmental conditions	Exposure duration (months)
Short term	ICTL00, ICTL0	----------	----------
Room ambient	ICTL2, ICTL4, ICTL8	Inside the lab	2, 4, 8
A	IA2, IA4, IA8	Outdoor (Tropical Climate)	2, 4, 8
B	IB2, IB4, IB8	Wet & dry in plain water	2, 4, 8
C	IC2, IC4, IC8	Submerged in plain water	2, 4, 8
D	ID2, ID4, ID8	Submerged in salt water (5%)	2, 4, 8
E	IE2, IE4, IE8	Submerged in acidic solution (4 < PH < 5)	2, 4, 8

radiation (UV) was investigated. According to the recorded data provided by Malaysian Meteorological Department, the temperature distribution was almost constant throughout the period of study between 20℃ and 34℃. The daily average temperature was recorded between 26℃ and 29℃ which shows a nearly steady temperature for the period of study. Besides, the relative humidity was recorded between 41% and 100% in this time. Meanwhile, the UV index was more than 8 degree for 15 days of the months in average.

Scenario (B) studied the influence of wet/dry cycles to find out the effect of rainy seasons on the bonding system. The exposure consisted of 1 week wet and 1 week dry in plain water inside room ambient. The aim of scenario (C) was to determine the influence of continuous moisture on the bonding system. In scenario (D) specimens were exposed to 5% salted water to study the effect of moisture accompanied with salt particles on the bonding behavior. Meanwhile, the pH value of both plain water and salt water was measured by around 8. Scenario (E) involved with the influence of acidic solution with the pH between 4 and 5 (The acidity of raining in the southern part of Malaysia) to simulate the effect of acid raining. For this purpose, sulphuric acid was added to the plain water and the pH of solution was measured with pH-meter every two weeks to maintain it constantly.

3.4 Test procedure and instrumentation

The beams were tested in four-point bending procedure with a 200 mm constant moment region (Fig. 1). The strengthened beams were simply supported using a spherically seated bearing and

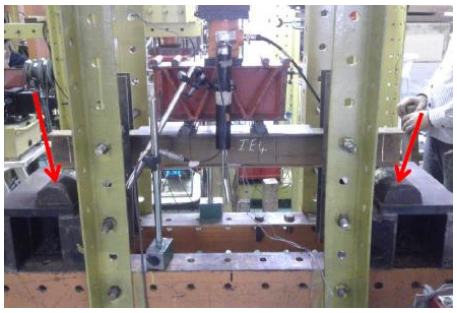

Fig. 2 Spherically seated supports

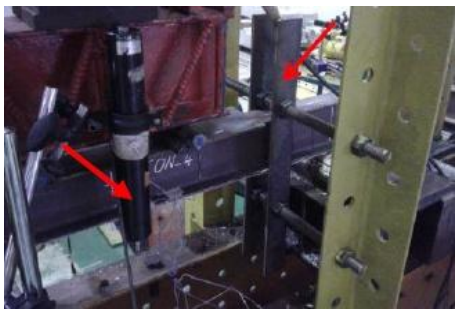

Fig. 3 Lateral supporting system, vertical LVDT

Fig. 4 Lateral LVDT

loaded under static loading as demonstrated in Fig. 2. The loading was applied using a hydraulic actuator and measured by a 300 kN load cell. In addition, a lateral supporting system was arranged to restrict the beams from moving laterally. Fig. 3 depicts these lateral supports. Two LVDT's were used to monitor the maximum deflection and lateral deformation of the mid-span as shown in Figs. 3- 4. Besides, distribution of stain in CFRP plate was obtained by installing strain gauges along the plate as shown in Fig. 1.

4. Test results and discussion

4.1 Mechanical properties of strengthened beam

Firstly, the mechanical properties of the strengthened beam was obtained and compared to the un-strengthened beam. For this purpose, bending tests were carried out and the load-deflection curves were potted for both beams as illustrated in Fig. 5. The graphs demonstrate a linear behavior in elastic region with a specific slope which proportional to the flexural stiffness (EI). For un-strengthened beam (ICTL00) the linear behavior continued until around 64.3 kN loading and 2.15 mm deflection which was considered as the yielding point. Then, the deflection increased rapidly until failure with a gradual loading enhancement. The ultimate load capacity and the maximum deflection were recorded approximately 82.6 kN and 32.1 mm, respectively. Besides, the flexural stiffness was obtained 29.9 kN/mm from the slope of the line between 20 to 60 kN loading. This means the un-strengthened steel beam showed a linear behavior in elastic region and a quite ductile behavior in plastic region until failure.

The same test was performed for the steel beam with CFRP strengthening at the bottom flange (ICTL0). Similarly, the load-deflection curve indicates linear behavior in elastic region as demonstrated in Fig. 5. Indeed, in elastic region the CFRP plate carried the load proportional to its section area and young's modulus. However, after steel yielding, more tensile stress was transferred to the CFRP plate immediately. When the bottom flange started to yield, the beam tended to deflect and rotate extremely at the mid-span as the plastic hinge started to form in this section. Nevertheless, the presence of CFRP plate had prevented the formation of large deflection. This effect caused improvement in the maximum elastic load capacity to around 88.2 kN which showed 37% increase. Further, the value of flexural stiffness increased approximately 13% to around 33.9 kN/mm.

The beam continued to carry additional load beyond the yielding point until failure. The ultimate load capacity reached to 117.8 kN which demonstrated about 43% increase. However, the maximum deflection declined to 19.23 mm and showed less ductility compared to beam ICTL00. Finally, failure happened suddenly in a brittle manner with a loud sound and debonding of the CFRP plate.

The failure mode of the strengthened beam was due to lateral-torsional buckling which finally led to global buckling. Lateral-torsional buckling is a limit-state of structural efficiency where the deformation of the beam changes from in-plane deflection to a combination of lateral deflection and twisting while the load capacity remains first constant before dropping off due to large deflections.

In addition, the load-deflection of these beams was calculated theoretically in elastic region to compare with the experimental results. The analysis of the stress-strain state of strengthened beam was carried out on the basis of the following main assumptions:

- Perfect bond between the steel beam and CFRP strengthening system;
- Plain sections remain plane after deformation;
- Negligible thickness of the strengthening system compare to the section depth;
- Negligible contribution of the adhesive layer to the stiffness of the member.

According to elastic theory of beam analysis, for a beam subjected to bending moment, the following equation defines flexural stress linearly distributed over the beam's cross section

$$\delta = M.\frac{y}{I} \tag{1}$$

Where M is the applied moment; y is the perpendicular distance from the neutral axis across of

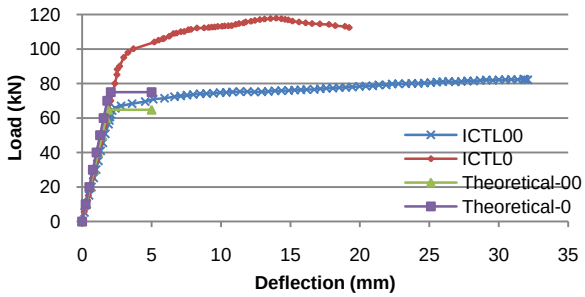

Fig. 5 Load-deflection of un-strengthened beam (CTIL00) and strengthened beam (ICTL0)

the beam section; *I* is the moment of inertia of the cross-sectional area and δ is the value of stress at distance *y* from neutral axis. After transforming the CFRP section using a modular ratio *n*, the location of the neutral axis *y* and the moment of inertia *I* of the transformed beam section can be determined using below equations

$$y = \sum \frac{y_i . A_i}{\sum A_i} \tag{2}$$

$$I = \sum \left(I_i + A_i . d_i^2 \right) \tag{3}$$

Where *yi*, Ai are distance for the centroid of each composite part and corresponding area; *Ii*, *di* are the moment of inertia of the composite part and the lever-arm distance. Besides, the maximum elastic deflection can be computed using Equation 4 as follow

$$\Delta = P . a \frac{(3L^2 - 4a^2)}{24EI} \tag{4}$$

Where *P* is the applied load, *L* is the free span beam length, *E* is the young's modulus and *a* is the distance of applied load and the beam end and as shown in Fig. 1. The result of theoretical analysis is represented in Fig. 5 as well. The graphs indicate the maximum elastic load and stiffness of the strengthened beam enhanced around 16% and 11%, respectively. However, in experimental results, these properties improved by 37% and 13%, respectively. It means, almost similar results were achieved by both methods for the beams stiffness. However, the elastic strength of the beams in theoretical analysis was more conservative than experimental method.

4.2 Test results of the exposed beams

The exposed beams were tested under the same four-point bending test at particular intervals to determine the effect of environmental conditions on the mechanical properties. For this purpose, the flexural behavior of these beams was investigated by comparing the mechanical properties with the control beam (ICTL0).

4.2.1 Failure mode of the exposed beams

The possible failure modes occurring in the strengthened steel beams with CFRP plate are as follows (National Research Council Advisory Committee 2007):

- Tension failure of steel beam or CFRP plate;
- Compression failure of steel beam (yielding or buckling);
- Delamination at the interface of CFRP and steel (debonding);
- Shear failure by local buckling at beam supports;
- Global buckling (axial or lateral-torsional) of the steel beam.

Basically, the failure mode for all the exposed beams in this study was due to lateral-torsional buckling as illustrated in Fig. 6. Although lateral supports prevent side deformation of the beam, but, rapid plastic displacement caused the beam to deform in a section between lateral support and end beam. After considerable lateral deformation of the beam, as the CFRP plate is not strong enough at the perpendicular direction, it was debonded instantly with a loud sound. Meanwhile, in

Fig. 6 Lateral-torsional buckling

Fig. 7 Longitudinal crack along CFRP plate

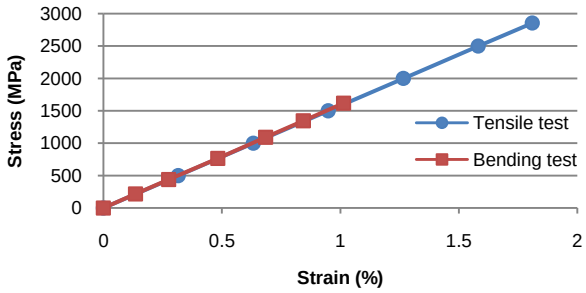

Fig. 8 Comparing stress-strain relationship of CFRP plate in tensile test and bending test

some cases the CFRP plate was split into two parts in longitudinal direction due to high shear stresses as shown in Fig. 7. This type of failure indicates the bonding system worked properly even after 8 month exposure in various environmental conditions. In fact, the steel plate at the top flange prevented the compression failure of steel beam. Further, the tensile stress of CFRP plate was lower than its maximum tensile capacity (as illustrated in Fig. 8) and therefore, it did not rupture by tension. In addition, proper treatment of the surfaces before bonding process caused appropriate contact between steel and CFRP plate and avoided the detrimental factors to influence the bonding strength significantly. Hence, the beams deformed out of section plane due to lateral-torsional buckling.

4.2.2 Mechanical properties of the strengthened beams after exposure

The load-deflection of the strengthened beams after 8 months exposure is presented in Fig. 9. The graphs indicate the behavior of the strengthened beams is essentially linear up to yielding of

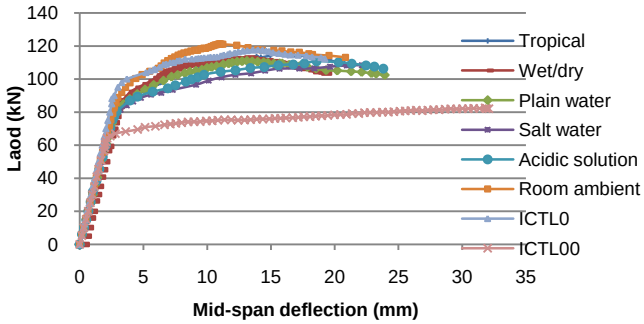

Fig. 9 Load-deflection of the strengthened beams after 8 months

the steel. Afterwards, it became increasingly non-linear until failure. In a short glance, the graphs demonstrate the strengthening system worked properly especially in elastic region. Evidently, for all environmental conditions the strengthening system increased the mechanical properties of the beams significantly compared to the un-strengthened specimen (ICTL00). However, in plastic region they behaved differently based on their exposures. In the following sections, the performance of strengthened beams in each environmental condition is explained separately and the results discussed in detail.

Room ambient

Fig. 10 illustrates the load-deflection and trend of changes in the mechanical properties of the beams in room ambient. The graphs indicate the flexural behavior of these beams in elastic and plastic region was relatively similar. Actually, the maximum elastic load of the beam after 2 months exposure increased slightly by 2% compared to control beam. However, gradual decrease around 3% and 5% occurred after 4 and 8 months of exposure, respectively. According to the graph, the elastic strength increased firstly because of post curing of the adhesive, but it decreased at the end of exposure. It means, subjecting to the room condition made a slow reduction in elastic strength.

Moreover, the flexural stiffness decreased compared to control beam 3-9%. In fact, subjecting to almost high humidity (70-90% RH) of room ambient caused softening of the adhesive and degraded the stiffness of the beams during exposure. Therefore, the maximum deflection increased from 19.23 mm to 20.85 mm at the end of aging. Meanwhile, the ultimate load capacity of the beams enhanced slightly about 2 to 4%. In fact, the ultimate load capacity changed slightly and if

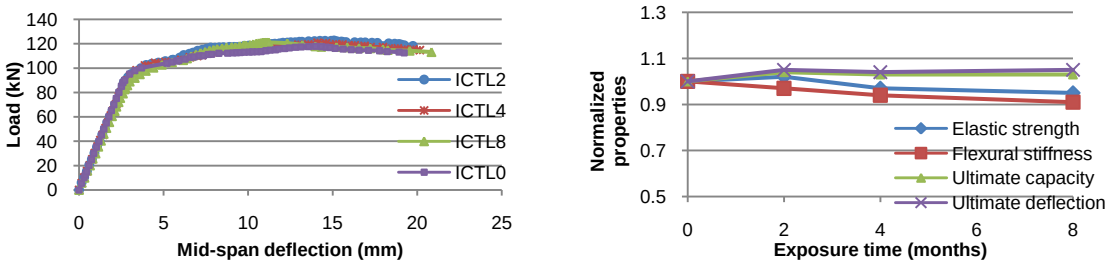

Fig. 10 Load-deflection and trend of changes in mechanical properties (room ambient)

the exposure time had been extended, it would decrease finally similar to other mechanical properties. Overall, the properties of strengthened beams in room ambient changed slightly during this period of time.

Natural tropical climate

Test results indicate both the elastic load capacity and the flexural stiffness increased around 1% after 2 months exposure to natural tropical climate. However, these properties decreased significantly after 4 and 8 months as it is shown in Fig. 11. These results confirm that high temperature of outdoor condition accelerated the adhesive polymerization process and caused the properties of the strengthened beam to be increased at the beginning of exposure. But, after finishing this process the outdoor environmental factors influenced the bonding properties and therefore affected the beam behavior. Besides, the adhesive behaved more ductile and made the ultimate deflection of the beam to be increased as well. The ultimate load capacity reduced around 2% at the end of exposure compared to the control beam (ICTL0).

Wet/dry condition

Fig. 12 depicts the load-deflection and the trend of changes in mechanical properties of the strengthened beams in wet/dry condition. The results demonstrate a gradual decrease in elastic strength for these beams. Referring to the graphs, the elastic strength decreased to 85.1, 83.2, and 81.4 kN after 8, 16, and 32 wet/dry cycles, respectively. However, the flexural stiffness increased in first 4 months around 4%. Indeed, water absorption and desorption influenced the epoxy adhesive during wet/dry exposure. This issue caused the adhesive stiffness to be enhanced at the beginning and the flexural stiffness of the beam increased as well. However, this environmental condition reduced the properties finally. Based on previous studies (Landrock 2009), micro cracks created in the adhesive layer gradually and made the properties to be reduced.

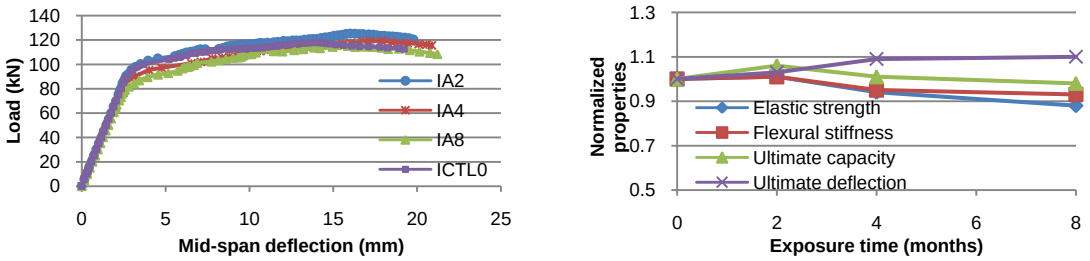

Fig. 11 Load-deflection and trend of changes in mechanical properties (outdoor condition)

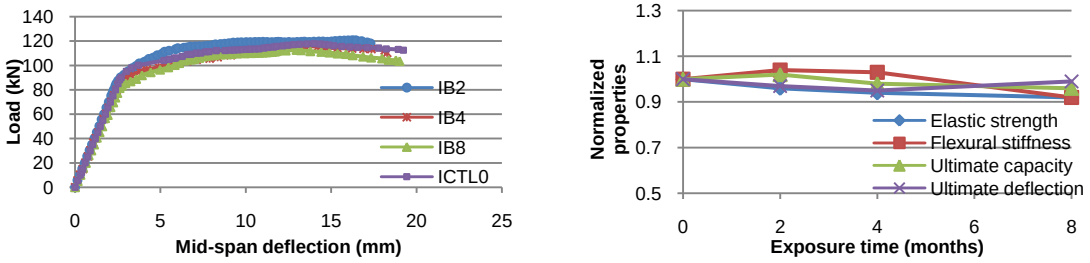

Fig. 12 Load-deflection and trend of changes in mechanical properties (wet/dry condition)

Immersion in plain water, salt water and acidic solution

The results show a noticeable decrease in the mechanical properties after exposure in plain water, salt water and acidic solution. In practice, water penetrates into the epoxy adhesive by diffusion or capillary action through cracks or porosity. Then, water molecules bond with the polymer via hydrogen bonding. Through this mechanism the water can disrupt the inter chain of Van Der Waals forces inside the network leading to increase of segmental mobility in long term. This issue is a form of chemical degradation and caused the properties to decrease significantly. Besides, swelling and plasticization of the adhesive due to moisture absorption influenced the properties and lead to more ductile behavior. Hence, the properties of strengthened beams were influenced by epoxy adhesive degradation. Meanwhile, the maximum deflection increased significantly and the beams behaved more ductile.

For the beams immersed in salt water, chemical attack due to the penetration of salt intensified the degradation and influenced the flexural behavior of the strengthened beam severely. Therefore, the most degradation of properties was observed for the beams subjected to salt water. The same results were extracted by Nguyen (Nguyen *et al*. 2012) for degradation of steel/CFRP double lap shear joints subjected to salt water. In addition, the properties of the beams subjected to acidic solution were almost similar to plain water beams. It means the effect of weak acidic solution considered as the same as plain water influence. Figs. 13-15 depict the load-deflection and trend of changes in mechanical properties of these beams. Table 5 summarizes the detail of mechanical properties at the end of conditioning for various exposures.

4.2.3 Ductility of strengthened beams after exposure

Ductility is defined as the "ability of material to undergo large deformations without rupture before failure". When ductile members are used to form a structure, the structure can undergo large deformations before failure (Gioncu *et al*. 2012). This is beneficial to the users of the structures,

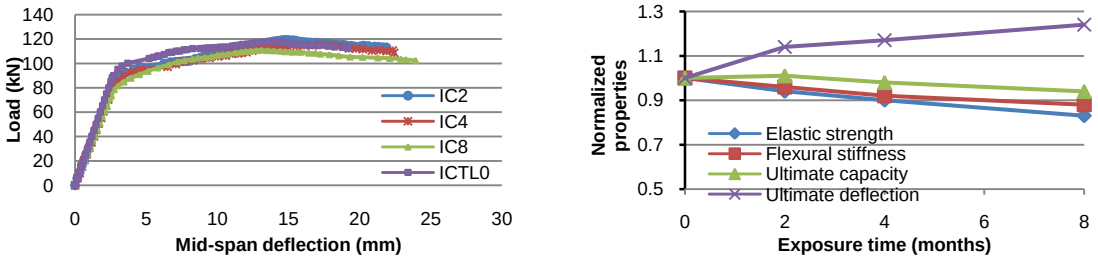

Fig. 13 Trend of changes in mechanical properties (immersed in plain water)

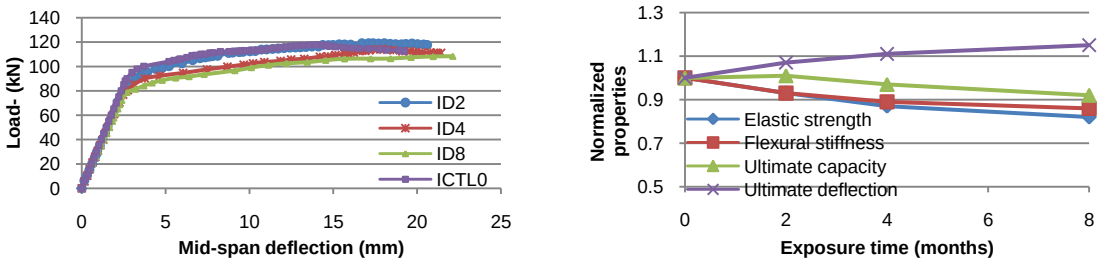

Fig. 14 Trend of changes in mechanical properties (immersed in salt water)

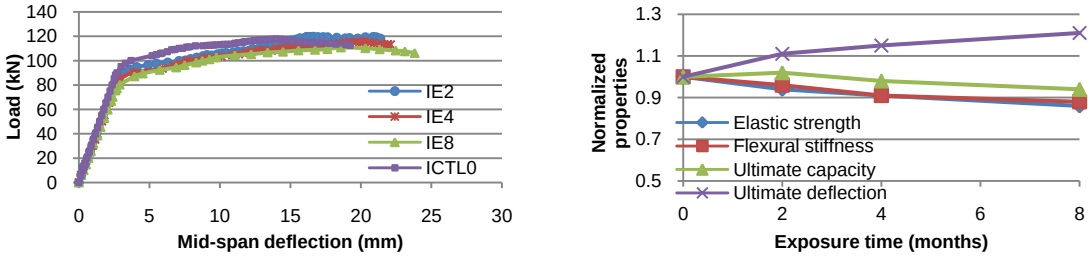

Fig. 15 Trend of changes in mechanical properties (immersed in acidic solution)

Table 5 The properties of strengthened beams after 8 months exposure to various environmental conditions

Scenario	Elastic load (KN)	Elastic stiffness (KN/mm)	Elastic deflection (mm)	Failure load (KN)	Ultimate deflection (mm)
Control	88.2	33.9	2.53	117.8	19.23
Room	83.8 (-5%)	30.8 (-9%)	2.73	121.1	20.85
Outdoor	77.2 (-12%)	31.5 (-7%)	2.48	115.7	21.21
Wet/dry	81.4 (-8%)	31.2 (-8%)	2.61	112.7	19.01
Plain water	73.5 (-17%)	29.8 (-12%)	2.55	110.9	23.93
Salt water	72.2 (-18%)	29.2 (-14%)	2.39	108.4	22.13
Acidic solution	75.5 (-14%)	29.8 (-12%)	2.59	110.8	23.82

as in the case of overloading and the structure is going to collapse; it will undergo large deformations before failure and thus provides warning to the occupants. This property is very important for structural members to be able to sustain loads over their maximum strength. There are two types of steel beam ductility which widely used in literature including "cross-section ductility" and "member ductility" (Gioncu and Mosoarca 2012). Cross-section ductility (or curvature ductility) refers to plastic deformation of cross-section while, member ductility (or rotation ductility) deals with loading system, beam span and cross-section of the beam. In this study, the member ductility was considered as a criterion to evaluate the ductility of the steel beams. The following equation was used to calculate the ductility of the beams

$$\xi = \frac{\Delta u - \Delta y}{\Delta y} \tag{5}$$

Where Δu and Δy are mid-span deflection at the ultimate load and yielding point, respectively and ξ is the beam ductility. According to investigation carried out by Gioncu and Mosoarca (2012), the ductility of steel beams is classified as presented in Table 6. Table 7 gives the ductility of strengthened beams based on above equation. Refer to mentioned classification all of the beams were classified as "medium ductile" member.

The strengthened beams showed more ductile behavior after exposure and the ultimate deformation increased gradually. Obviously, the strengthened beams subjected to the moisture condition (scenarios C, D and E) displayed more ductility. The main reason was reduction of shear modulus due to swelling and softening of the adhesive leading to more deformation of the beams before failure. On the other hand, the beams exposed to outdoor exposure demonstrated less

Table 6 Classification of steel beams based on ductility

Classification	Ductility
High ductility	ξ >7.5
Medium ductility	4.5< ξ <7.5
Low ductility	1.5< ξ <4.5
Non-ductile	ξ <1.5

Table 7 Ductility of exposed beams (8 months exposure)

Scenario	Specimen	Elastic deflection (mm)	Ultimate deflection (mm)	Ductility
Un-strengthened beam	ICTL00	2.15	32.10	13.9
Control beam	ICTL0	2.60	19.23	6.4
Room ambient	ICTL8	2.73	20.85	6.6
Tropical climate	IA8	2.48	21.21	7.6
Wet/dry	IB8	2.61	19.01	6.3
Plain water	IC8	2.55	23.93	8.4
Salt water	ID8	2.39	22.13	8.3
Acidic solution	IE8	2.59	23.82	8.2

ductility. Indeed, thermal cycles and humidity variation caused the adhesive to be more brittle and therefore the flexural stiffness of the beams increased gently. In summary, strengthening of steel beams indicated a proper ductility even after exposure to various environmental conditions.

4.2.4 Shear stress in adhesive layer

Distribution of shear stress in the adhesive layer is a vital issue to study the behavior of bonding after exposure. Indeed, the value of shear stress which is transferred by the adhesive indicates the durability strength of the bonding. For this purpose, the strain gauges were installed along CFRP plate. Hence, four regions were formed from mid-span to the end plate with the distance of 100 mm. The distribution of strain along CFRP plate for control beam is represented in Fig. 16. The graphs demonstrate the strain rate was almost linearly constant in the beginning of loading (50 kN). However, it increased significantly in the middle of CFRP plate at higher load levels and became non-linear which shows the stress transferred to the strengthening system through the bonding.

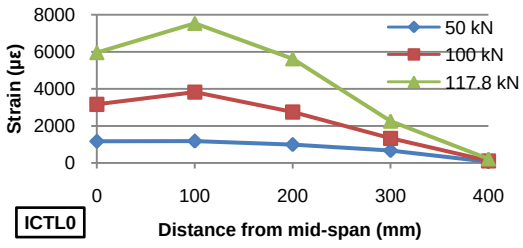

Fig. 16 Strain distribution along CFRP plate for control beam

Normally, the maximum strain formed at the bottom of point load before failure and decreased towards the end of CFRP plate which was similar to the results obtained by Schnerch *et al*. (2007). The same trend of strain distribution occurred for all the exposed beams. Comparing the results for each condition indicated when the time of exposure increased, the maximum strain decreased gradually. Evidently, the maximum strain was proportional to the ultimate load capacity of the beam.

The shear stress in the adhesive layer was determined using Eq. (6) as follow

$$\tau = \frac{\Delta\varepsilon}{\Delta x}.E_c.t_c \tag{6}$$

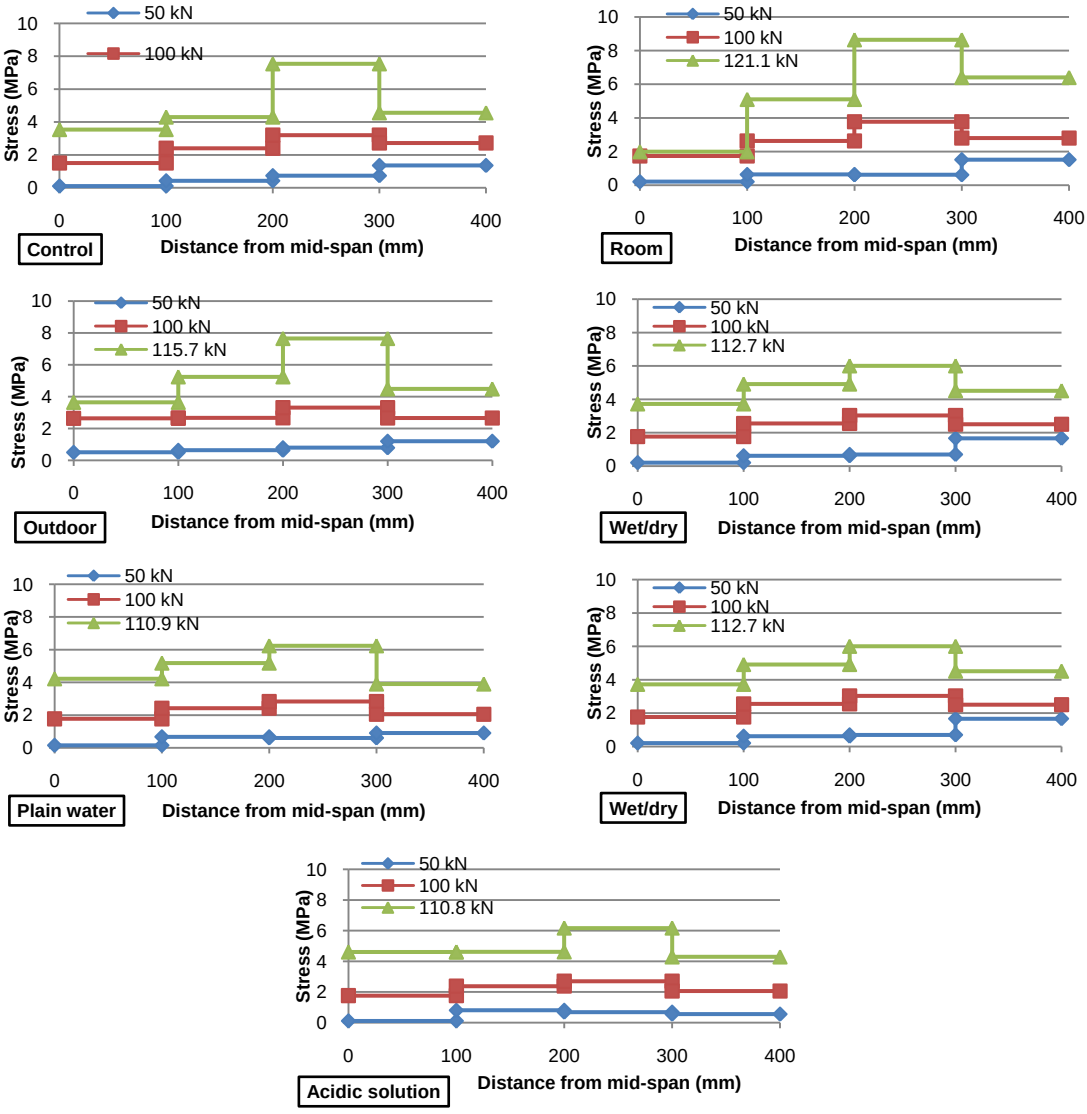

Fig. 17 Shear stress distribution in the adhesive layer (along CFRP plate) in various environmental conditions after 8 month exposure

Table 8 Shear stress in adhesive layer along CFRP plate at failure load

Beam code	Ultimate load capacity (kN)	Shear stress in adhesive layer at failure load (MPa)				Average shear stress (MPa)
		0-100 (mm)	100-200 (mm)	200-300 (mm)	300-400 (mm)	
ICTL0	117.8	3.54	4.30	7.54	4.56	4.99
ICTL8	121.1	2.81	5.10	8.64	6.40	5.74
IA8	115.7	3.64	5.24	7.65	4.48	5.25
IB8	112.7	3.73	4.92	6.01	4.52	4.79
IC8	110.9	4.22	5.18	6.24	3.90	4.89
ID8	108.4	4.17	4.75	6.33	3.91	4.79
IE8	110.8	4.61	4.62	6.17	4.29	4.92

where $\Delta\varepsilon$ is the difference of longitudinal strain in two consecutives strain gauge; Δx is the distance between two consecutive strain gauge (mm); *Ec* , *tc* are young modulus and thickness of CFRP plate, respectively and τ is the shear stress in adhesive layer. Shear stress distribution along the CFRP plate for the beams in various conditions (8 months exposure) is illustrated in Fig. 17.

The graphs demonstrate the shear stress has been distributed almost uniformly along the strengthening plate at the load level lower than maximum elastic load (50 kN). Further, the maximum shear stress formed at the end of the CFRP plate and decreased gradually towards mid-span in this load level. As the stress distribution became non-uniform at higher load levels, the maximum stress shifted from region 4 (300-400 mm) to region 3 (200-300 mm).

Comparing the results for the beams with different exposure period revealed that by increasing the time of exposure, the maximum shear stress in the adhesive layer decreased gradually. This means the degradation of adhesive properties caused lower stress transferring to the CFRP plate and therefore the mechanical properties of the beams decreased at the end. In addition, the graphs represent the maximum stress occurred for the beams subjected to room ambient and outdoor environment around 8 MPa. As already discussed, post curing of the epoxy adhesive in these conditions caused the capacity of the beams to be improved and the shear stress increased along the adhesive layer. Nevertheless, in Scenarios B, C, D and E the maximum shear stress was recorded around 6 MPa, because of quick detrimental effects on the epoxy adhesive properties. Table 8 gives the detail of shear stress along the CFRP plate for the exposed beams (8 months exposure) at failure load. Based on the results, the maximum and minimum shear stress were recorded for the outdoor beam (IA2) and the beam immersed in salt water (ID8), respectively.

Overall, the results indicate in elastic range the shear stress along the adhesive layer was nearly the same for all the beams. However, at higher load levels the bonding was influenced by the exposure and therefore transferred lower stress to the CFRP plate.

4.3 Properties of CFRP coupons after exposure

The mechanical properties of CFRP plate was evaluated individually. For this purpose, tensile test was conducted on the CFRP coupons which were exposed to the same environmental conditions. The properties evaluation was made by comparison between the control and exposed specimens to identify the effect of exposure condition. The exposed CFRP coupons were taken out from the designated exposure regime at defined intervals.

The results of tensile tests indicate the degradation of mechanical properties of CFRP coupons

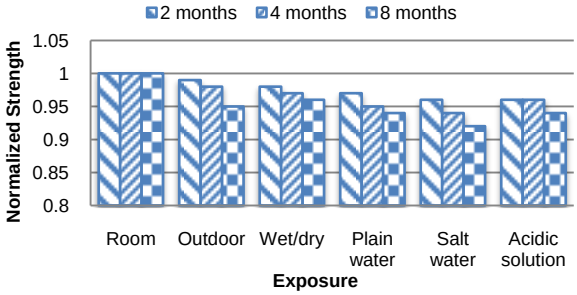

Fig. 18 Normalized strength degradation of CFRP coupons in various environmental conditions

was negligible during this period of time as represented in Fig. 18. Basically, the tensile strength and stiffness were mainly governed by the properties of the fibers which were affected very slightly. The strength degradation was almost the same as the results reported by Nguyen *et al*. (2012), but, the stiffness reduction was a little more. The most reduction of strength and stiffness was recorded for salt water condition around 8% and 6%, respectively. Obviously, the penetration of salt accompanied with moisture and chemical attack of chloride ions might cause such degradation on the specimens.

4.4 Properties of epoxy adhesive coupons after exposure

The epoxy adhesive coupons were prepared and subjected to the same environmental condition and tested at the same intervals to be assessed individually. There are a number of semi-empirical relationships to predict the degradation process of the polymer material. These are usually of the form

$$P_t = (P_0 - P_\infty)\, exp(kt) + P_\infty \tag{7}$$

Where t is the aging time, P_t, P_0, P_∞ are properties of the material in time (t) and ($t = 0$) and ($t = \infty$), respectively, and k is the rate of degradation. This model was developed by Phani and Bose (1987) and also was employed by Nguyen *et al*. (2012) to study the effect of moisture and temperature on the properties of DLS joints.

In this method, it is required to predict the maximum degradation of the properties by using an accelerated test. Hence, epoxy adhesive dog-bone coupons were prepared and subjected to 55℃ plain water to find the maximum degradation of mechanical properties P_∞. The results of the tensile tests indicated the maximum reduction of 39% and 47% for strength and stiffness, respectively. By using Eq. (7) and regression analysis, the rate of degradation k was calculated for these specimens approximately -0.03352 mm^2/day. The same technique was used to model the stiffness degradation of the epoxy adhesive. The results are summarized in Table 9.

Table 9 The values of parameters for strength and stiffness modeling

Environment	Modeling strength			Modeling stiffness		
	P_0 (%)	P_∞ (%)	k (mm^2/day)	P_0 (%)	P_∞ (%)	k (mm^2/day)
Plain water (55℃)	100	61	-0.03352	100	53	-0.03955

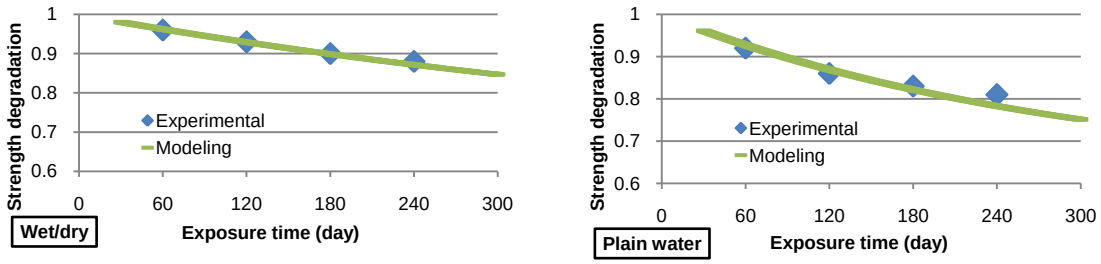

Fig. 19 Comparing experimental and modeling degradation of epoxy adhesive

Table 10 Degradation rate of epoxy adhesive in various environmental conditions

Scenario	Strength degradation rate (mm^2/day)	Stiffness degradation rate (mm^2/day)
Tropical climate	-0.000729	-0.000232
Wet/dry	-0.001658	-0.000916
Plain water	-0.003374	-0.004861
Salt water	-0.005144	-0.003908
Acidic solution	-0.003986	-0.002487

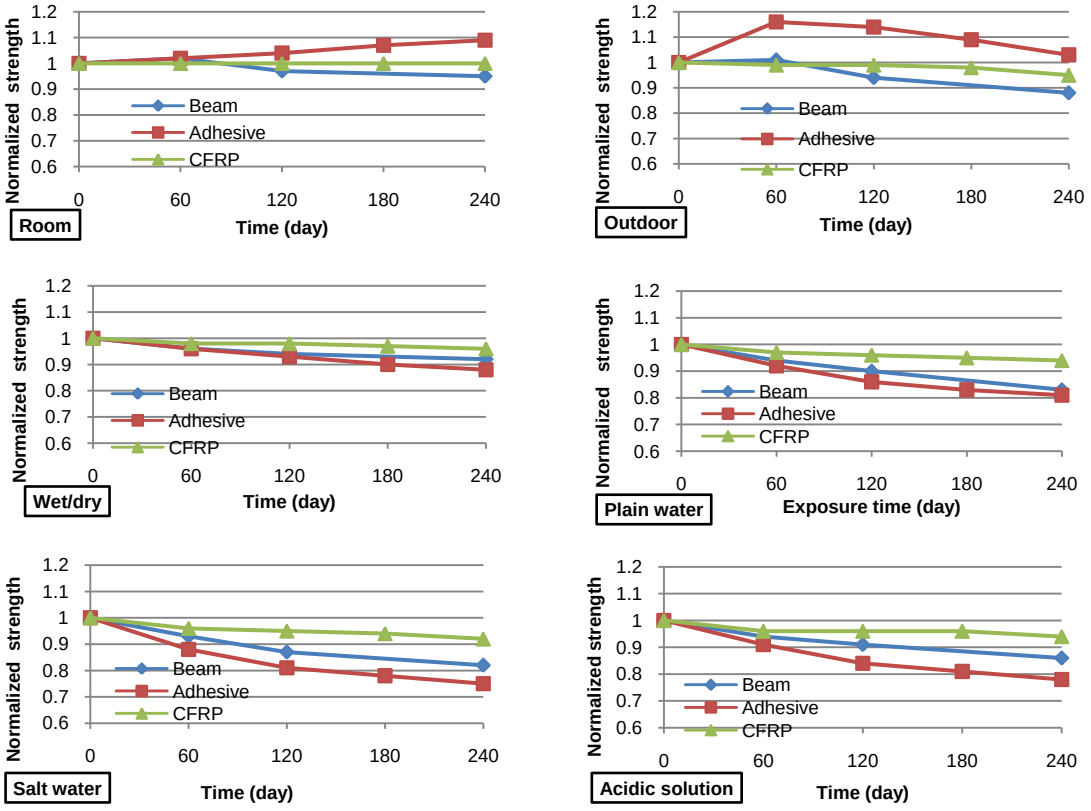

Fig. 20 Comparing the trend of changes in strength of beams, epoxy adhesive and CFRP

Similar technique was used to find the rate of degradation for other conditions. Fig. 19 compares the results of experimental program and the analytical modeling for wet/dry cycles and plain water condition. It can be seen the results demonstrate appropriate conformity. Table 10 gives the rate of degradation for various environmental conditions. It shows clearly that the degradation rate of the samples for the tropical climate environment is pretty low compared to other exposure conditions. The most rate of strength degradation was determined for salt water approximately 0.005144 mm^2/day. In addition, plain water condition was found to be the most stiffness degradation for epoxy adhesive coupons with the rate of -0.004861 mm^2/day.

In addition, the trend of changes in the strength of the beams and epoxy adhesive in diverse environmental exposures compared together as illustrated in Fig. 20. Evidently, in room ambient the strength of specimens was almost constant during the period of study. However, in tropical climate the strength of both specimens increased at the beginning and then decreased gradually. Moreover, in wet/dry cycles, plain water, salt water and acidic solution the strength decreased significantly. The graphs shows the epoxy adhesive coupons were influenced more severely than strengthened beams. Obviously, all surfaces of the coupons were affected by the aging, while for the beams the adhesive layer surfaces were confined by steel and CFRP plate.

In summary, the trend of changes in the properties of strengthened beams and epoxy adhesive coupons were relatively similar. These results indicate the flexural properties of the strengthened beams were mainly related to the epoxy adhesive behavior. In other words, reduction of strength and stiffness of the adhesive due to detrimental effects caused decreasing of the strengthening system properties.

5. Conclusions

The use of CFRP plate has been demonstrated as a successful technique to increase the mechanical properties of the steel elements. The main limitation of this technique has been the durability of bonding system in various environmental conditions. The focus of current research was to investigate the performance of steel/CFRP strengthening system in various environmental conditions. I-section steel beams were strengthened with CFRP pultruded plate and subjected to various conditions. Then, the mechanical properties were compared with the unexposed specimens to find the performance of the bonding system. Besides, the properties of the CFRP and epoxy adhesive were investigated individually. The study found that the CFRP plate was a superior durable material which is suitable for strengthening of steel elements. Overall, the following conclusions are drawn from the study:

- The performance of strengthened beams was mainly governed by the epoxy adhesive properties. Reduction of strength and stiffness of the epoxy adhesive was found to be the critical part and the performance of the system is related directly to its behavior during exposure.
- The experimental results indicated that the maximum elastic load and ultimate load capacity of the strengthened beam increased 37% and 43%, respectively compared to un-strengthened beam. Besides, the flexural stiffness improved approximately 13%. However, the ultimate deflection decreased significantly and therefore the ductility decreased after strengthening.
- The failure mode for all exposed strengthened beams was lateral-torsional buckling which showed the strength of bonding was still appropriate after exposure to various

environmental conditions.

- The ductility of the exposed strengthened beams was found to be increased after exposure. Basically, the stiffness of the adhesive reduced after exposure due to moisture absorption and caused the beams to behave in a more ductile manner.
- The strength and stiffness of the beams in room ambient were almost constant. However, for the outdoor beams improved slightly in first 2 months and then decreased gradually until the end of exposure. High temperature and humidity, wet/dry cycles and UV radiation influenced the properties of bonding in this duration gently.
- The mechanical properties of the strengthened beams which were immersed in plain water, salt water and acidic solution decreased almost in the same trend. The highest degradation of 18% was observed for the beams immersed in salt water. Indeed, penetration of the slat and chemical attack of chloride ions caused this reduction in properties.
- The tensile stress along the CFRP plate for all the strengthened beams was almost similar in elastic range. In addition, the maximum strain occurred at the bottom of point load at failure load for all the beams tested. Likewise, the shear stress distributed uniformly in the adhesive layer at the load levels lower than maximum elastic load. However, at higher load levels it changed to a quite non-uniform distribution.
- A theoretical method was employed to estimate the degradation of mechanical properties of epoxy adhesive. The modeling curves compared well with the experimental results. The rate of degradation was calculated for each condition and concluded in tropical climate the epoxy adhesive properties decreased slowly compared to other exposures. Besides, the most degradation of strength and stiffness was obtained for salt water and plain water, respectively.

Acknowledgments

The authors wish to acknowledge Civil Engineering Faculty and Construction Research Center (CRC) for their assistance in conducting the tests at University Technology Malaysia (UTM). The authors would also like to appreciatively acknowledge support provided through Grant No: Q.J130000.2517.07H32 from Research Management Center (RMC).

References

Al-Saidy, A., Klaiber, F. and Wipf, T. (2007), "Strengthening of steel-concrete composite girders using carbon fiber reinforced polymer plates", *Construct. Build. Mater.*, **21**(2), 295-302.

Al-Zubaidy, H., Al-Mahaidi, R. and Zhao, X. (2013), "Finite element modelling of CFRP/steel double strap joints subjected", *Compos. Struct.*, **99**, 48-61.

ASTM (2008), Standard Test Method for Tensile Properties of Polymer Matrix Composite Materials; American Society for Testing and Materials, PA, USA.

ASTM (2010), Standard Test Method for Tensile Properties of Plastics; American Society of Testing and Materials, PA, USA.

ASTM (2012), Standard Test Methods and Definitions for Mechanical Testing of Steel Products; American Society for Testing and Materials, PA, USA.

Colombi, P. and Fava, G. (2012), "Fatigue behaviour of tensile steel/CFRP joints", *Compos. Struct.*, **94**(8), 2407-2417.

Colombi, P. and Poggi, C. (2006), "An experimental, analytical and numerical study of the static behavior of

steel beam reinforced by pultruded CFRP strips", *J. Compos.*: *Part B*, **37**(1), 64-73.
Cromwell, J., Harries, K. and Shahrooz, B. (2011), "Environmental durability of externally bonded FRP materials intended for repair of concrete structures", *Construct. Build. Mater.*, **25**(5), 2528-2539.
Dawood, M. and Rizkalla, S. (2010), "Environmental durability of a CFRP system for strengthening steel structures", *J. Construct. Build. Mater.*, **24**(9), 1682-1689.
Deng, J. and Lee, M. (2007), "Behaviour under static loading of metallic beams reinforced with a bonded CFRP plate", *Compos. Struct.*, **78**(2), 232-242.
Malaysian Meteorological Department; http://www.met.gov.my
Gholami, M., Mohd Sam, A., Mohamad Yatim, J. and Md Tahir, M. (2013), "A review on steel/CFRP strengthening systems focusing environmental performance", *Construct. Build. Mater.*, **47**, 301-310.
Gioncu, V. and Mosoarca, M. (2012), "Ductility aspects of steel beams", *Civil Eng. Architect.*, **55**(1), 37-60.
Gioncu, V., Mosoarca, M. and Anastasiadis, A. (2012), "Prediction of available rotation capacity and ductility of wide-flange beams: Part 1: DUCTROT-M computer program", *J. Construct. Steel Res.*, **69**(1), 8-19.
Hollaway, L. (2010), "A review of the present and future utilization of FRP composites in the civil infrastructure with reference to their important in-service properties", *Construct. Build. Mater.*, **24**(12), 2419-2445.
Kabir, M. and Eshaghian, M. (2010), "Flexural upgrading of steel-concrete composite girders using externally bonded CFRP reinforcement", *Appl. Compos. Mater.*, **17**(2), 209-224.
Kim, Y. and Brunell, G. (2011), "Interaction between CFRP-repair and initial damage of wide-flange steel beams subjected to three-point bending", *Compos. Struct.*, **93**(8), 1986-1996.
Kim, Y., Hossain, M. and Yoshitake, I. (2012), "Cold region durability of a two-part epoxy adhesive in double-lap shear joints: Experiment and model development", *Construct. Build. Mater.*, **36**, 295-304.
Kumar, S., Sridhar, I. and Sivashanker, S. (2008), "Influence of humid environment on the performance of high strength structural carbon fiber composites", *Mater. Sci. Eng. A*, **498**(1-2), 174-178.
Landrock, A. (2009), *Adhesives Technology Handbook*, William Andrew, London, UK.
Lettieri, M. and Frigione, M. (2012), "Effects of humid environment on thermal and mechanical properties of a cold-curing structural epoxy adhesive", *Construct. Build. Mater.*, **30**, 753-760.
Mertz, D. and Gillespie, J. (2002), *The Rehabilitation of Steel Bridge Girders using Advanced Gomposite Materials*, National Research Council; Transportation Research Board, Washington, D.C., USA.
Narmashiri, K. and Jumaat, M. (2011), "Reinforced steel I-beams: A comparison between 2D and 3D simulation", *Simul. Model. Practice Theory*, **19**(1), 564-585.
Narmashiri, K., Jumaat, M. and Sulong, R. (2010), "Shear strengthening of steel I-beams by using CFRP strips", *Scientif. Res. Essays*, **5**(16), 2155-2168.
National Research Council Advisory Committee (2007), Guidelines for design and construction of externally bonded FRP systems for strengthening existing structures-metallic structures, National Research Council, Rome, Italy.
Nguyen, T., Bai, Y., Zhao, X. and Al-Mahaidi, R. (2011), "Mechanical Characterization of steel/CFRP double strap joints at elevated temperature", *Compos. Struct.*, **93**(6), 1604-1612.
Nguyen, T., Bai, Y., Zhao, X. and Al-Mahaidi, R. (2012), "Durability of steel/CFRP double strap joints exposed to sea water, cyclic temperature and humidity", *Compos. Struct.*, **94**(5), 1834-1845.
Patnaik, A., Bauer, C. and Srivastan, T. (2008), "The extrinsic influence of carbon fiber reinforced plastic laminates to strengthen steel structures", *Sadhana*, **33**(3), 261-272.
Phani, K. and Bose, N. (1987), "Temperature dependence of hydrothermal ageing of CSM-laminate during water immersion", *Compos. Sci. Technol.*, **29**(2), 79-87.
Schnerch, D., Dawood, D., Rizkalla, S. and Sumner, E. (2007), "Proposed design guidelines for strengthening of steel bridges with FRP materials", *Construct. Build. Mater.*, **21**(5), 1001-1010.
Seleem, M., Sharaky, I. and Sallam, H. (2010), "Flexural behavior of steel beams strengthened by carbon fiber reinforced polymer plates – Three dimensional finite element simulation", *Mater. Des.*, **31**(3), 1317-1324.
Sen, R., Liby, L., Spillet, K. and Mullins, G. (1995), "Strengthening steel composite bridge members using

CFRP laminates", *Proceedings of the 2nd International RILEM Symposium*, London, UK, August.
Sen, R., Liby, L. and Mullins, G. (2001), "Strengthening steel bridge sections using CFRP laminates", *Compos*.: *Part B*, **32**(4), 309-322.
Shan, L., Hui-Tan, R., Yi-Yan, L. and Mu-Huan, S. (2011), "Environmental degradation of carbon fiber reinforced polymer (CFRP) and steel bond subjected to hygrothermal aging and loading", *Mater*. *Sci*. *Forum*, 559-562.
Stratford, T. and Bisby, L. (2012), "Effect of warm temperatures on externally bonded FRP strengthening", *J*. *Compos*. *Construct*., **16**(3), 235-244.
Zhou, H., Attard, T., Wang, Y., Wang, J. and Ren, F. (2013), "Rehabilitation of notch damaged steel beams using a carbon fiber reinforced hybrid polymeric-matrix composite", *Compos*. *Struct*., **106**, 690-702.

CC